SUPPLEMENTAL INFORMATION

A

	genotype	stage	DA1nuclei
A	Control *foi* ^{C887}/*TM3*	16	12.4± 0.4 (n=55)
B	*foi* ^{C887}	16	5.1± 0.5 (n=59)
C	*UASLIV1/+; Mef2Gal4foi*^{C887}*/foi*^{C887}	16	8.5± 0.5 (n=37)
D	*UASCatsup/+; Mef2Gal4foi*^{C887}*/foi*^{C887}	16	6.0± 0.7 (n=35)
E	*UASZip42C/+; Mef2Gal4foi*^{C887}*/foi*^{C887}	16	9.6± 0.8 (n=28)
F	*UASZip71B/+; Mef2Gal4foi*^{C887}*/foi*^{C887}	16	3.8± 0.5 (n=27)
G	*UASZip71B/+; Mef2Gal4foi*^{C887}*/foi*^{C887}(25°)	16	7.8± 0.5 (n=31)
H	*UASZip71B/+; Mef2Gal4foi*^{C887}*/+*	16	4.8± 0.5 (n=41)

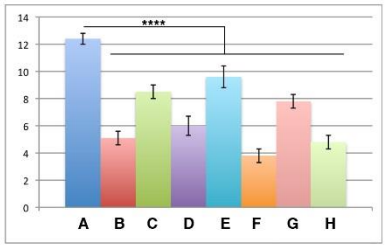

B

	genotype	stage	Twi-nuclei
A	*foi*^{C887}*/TM3*	13	6.3 ± 0.3 (n=10)
B	*foi*^{C887}	13	25.6 ± 2.0 (n=27)
C	*UASfoi;foi*^{C887}	13	18.0 ± 1.8 (n=9)
D	*UASfoi/+; Mef2Gal4foi*^{C887}*/foi*^{C887}	13	7.0 ± 0.5 (n=16)
E	*UASfoi/+; snsGal4foi*^{C887}*/foi*^{C887}	13	8.7 ± 0.9 (n=16)
F	*UASfoi/+; dufGal4foi*^{C887}*/foi*^{C887}	13	13.5 ± 1.3 (n=19)
G	*UASCatsup/+; Mef2Gal4foi*^{C887}*/foi*^{C887}	13	20.0 ± 1.3 (n=9)
H	*UASLIV1/+; Mef2Gal4foi*^{C887}*/foi*^{C887}	13	27.7 ± 2.5 (n=14)
I	*UASZip42C/+; Mef2Gal4foi*^{C887}*/foi*^{C887}	13	6.9 ± 0.4 (n=17)
J	*UASZip71B/+; Mef2Gal4foi*^{C887}*/foi*^{C887}	13	7.3 ± 0.6 (n=15)
K	*Mef2Gal4foi*^{C887}*/UASZnT1foi*^{C887}	13	27.4 ± 1.9 (n=15)
L	*UASminc/+; Mef2Gal4foi*^{C887}*/foi*^{C887}	13	23.8 ± 1.9 (n=31)
M	*minc*^{A388}	13	32.4 ± 1.3 (n=30)

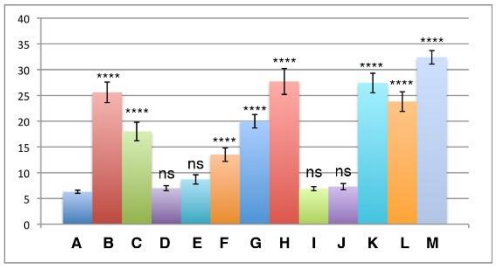

FIGURE S1, related to Figures 3, 6. Quantification of Eve-expressing DA1 nuclei and Twi nuclei in different genetic combinations of *foi*

The figure shows the number of Eve-expressing nuclei in DA1 muscles (A) and Twi-expressing nuclei (B) in embryos at developmental stages 16 (A) or 13 (B) of the indicated genotypes. (*n*, number of hemisegments quantified). Error bars as CI

****P<0.0001 (one-way ANOVA test).

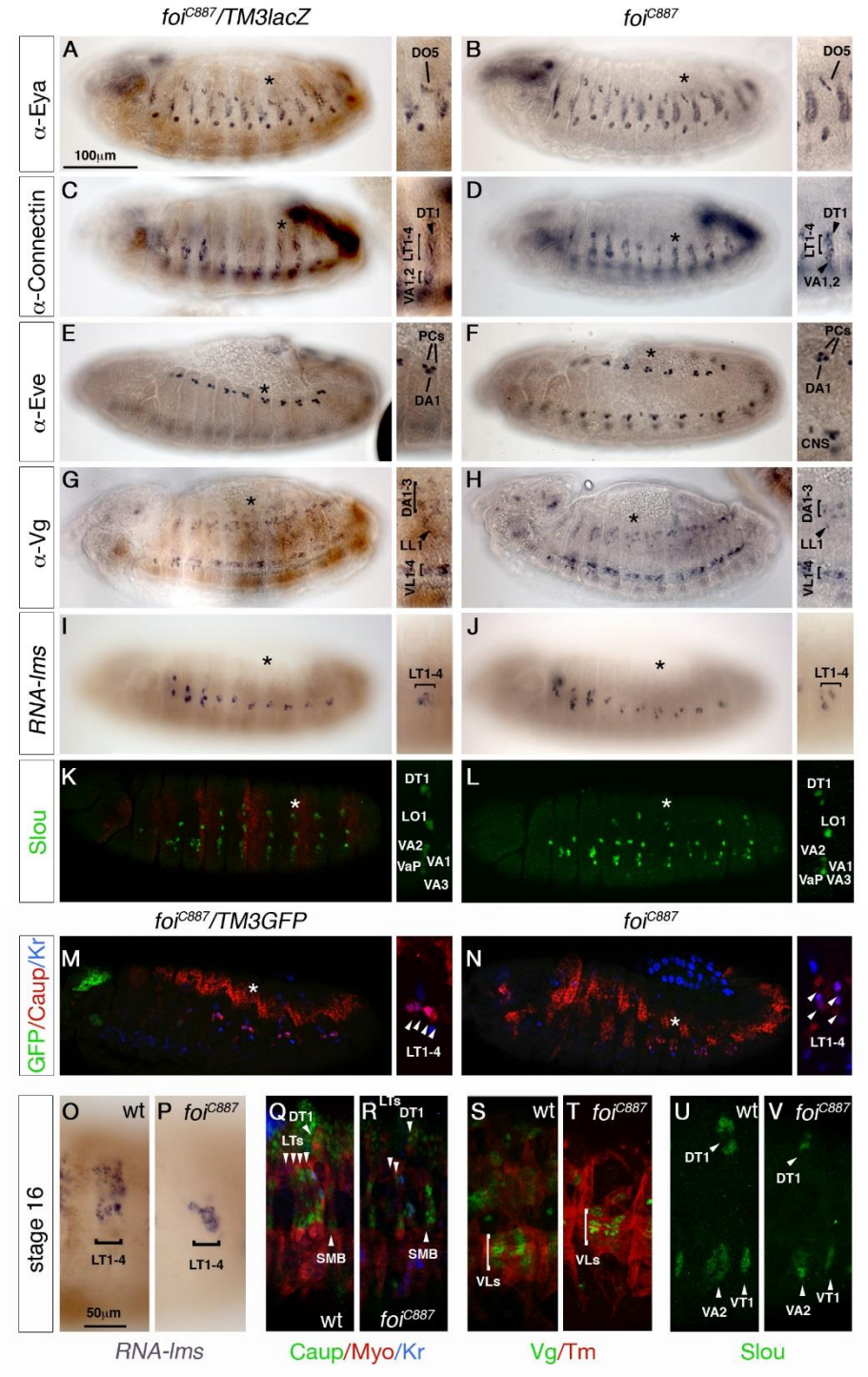

FIGURE S2, related to Figure 2. wild-type and *foi* FCs express the same code of muscle identity genes

(A-N) Lateral views of stage 12-14 control (left column) and *foi* ^{C887} embryos (right column) stained with probe or antibodies for different FC markers as indicated in the

left margin. The magnifications correspond to the hemisegment marked by an asterisk in the corresponding embryo, and show the relevant muscles stained with the different antibodies or probe. Note that the expression of muscle marker genes is initiated properly in *foi* mutants although muscles contain fewer nuclei due to the fusion defect. (O-V) Details of the lateral regions of stage 16 control and *foi* mutant embryos stained with probe or antibodies for FC markers as indicated. The confocal images show Z projections of several consecutive sections.

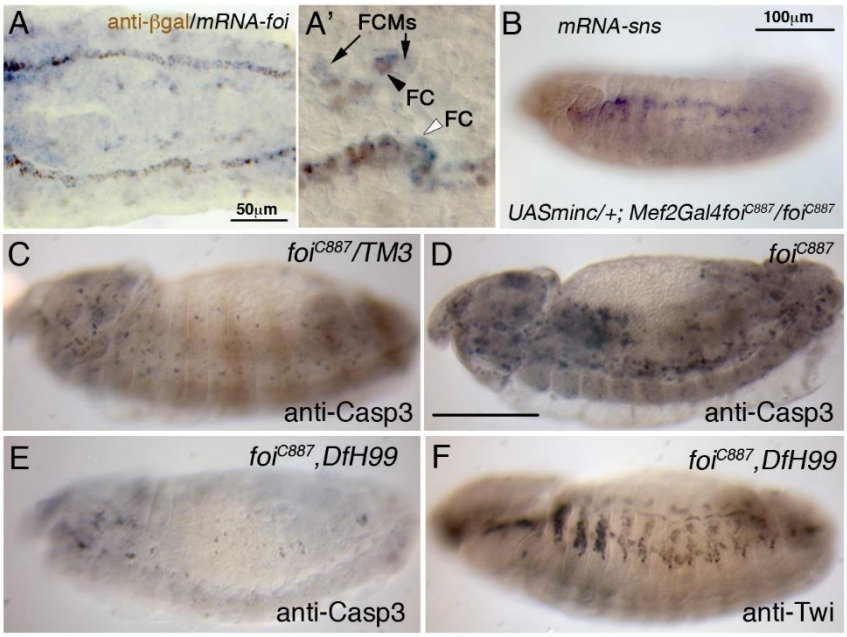

FIGURE S3, related to Figures 2, 3. The blockade of myogenic differentiation in *foi* FCMs causes their elimination by apoptosis

(A, A') ventral view of a *rP298* stage 11 embryo showing that *foi* transcripts accumulate in somatic and visceral founders (FC, black and white arrowheads in A') and in fusion-competent myoblasts (FCMs, arrows in A'). (B) Over-expression of *minc* in the mesoderm of *foi* embryos cannot restore *sns* expression. (C-E) Lateral views of stage 14 control (C), *foi*^{C887} (D) and *foi*^{C887} *DfH99* (E) embryos stained with an antibody to activated Caspase 3. Note the large number of apoptotic FCMs in *foi* ^{C887} embryos that are not seen in *foi* ^{C887} *DfH99*. (F) Lateral view of a stage 14 *foi*^{C887} *DfH99* embryo stained with anti-Twist to show the faulty differentiation of FCMs.

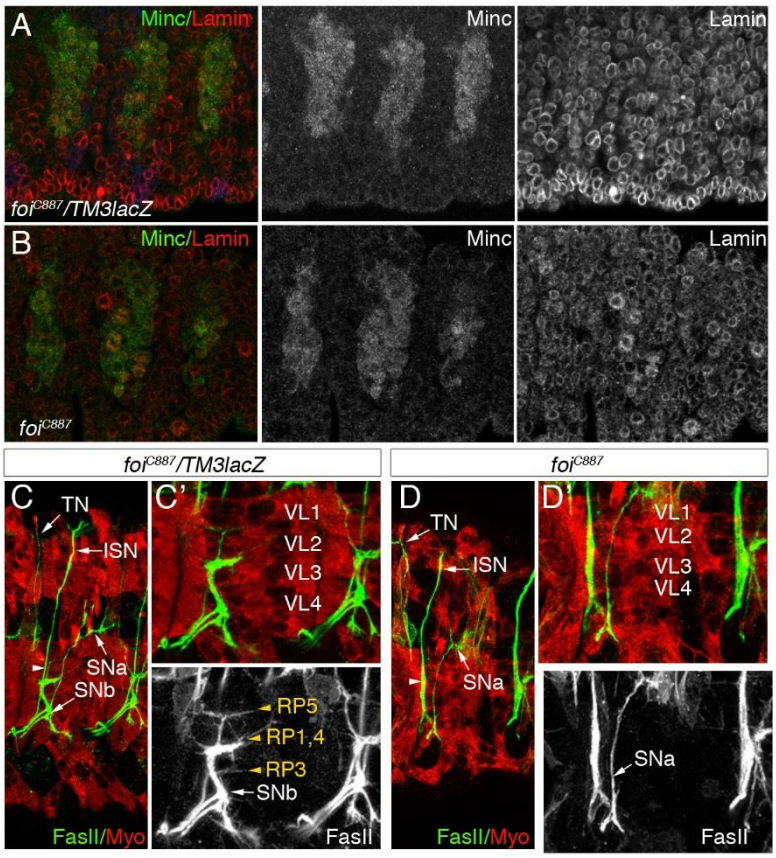

FIGURE S4, related to Figure 2. Minc subcellular localization and innervation defects in *foi* mutants

(A, B) Lateral views of three abdominal segments of stage 14 control (*foi*^{C887}*/TM3lacZ*, A) and *foi*^{C887} (B) embryos stained with antibodies against Minc (green) and Lamin (Red) to label the nuclear membrane. In both genotypes Minc protein is found in the nuclei and cytoplasm. (C-D') Ventro-lateral regions of control (*foi*^{C887}*/TM3lacZ*, C) and *foi*^{C887} (D) late stage 16 embryos stained with anti Myosin (red) and anti-FasII (green) to reveal the peripheral motor projections. In *foi* mutants the SNb branch does not defasciculate from the dorsal ISN leaving ventral muscles without innervation. Note the thickening of the ISN in D (arrowhead, compare to C).

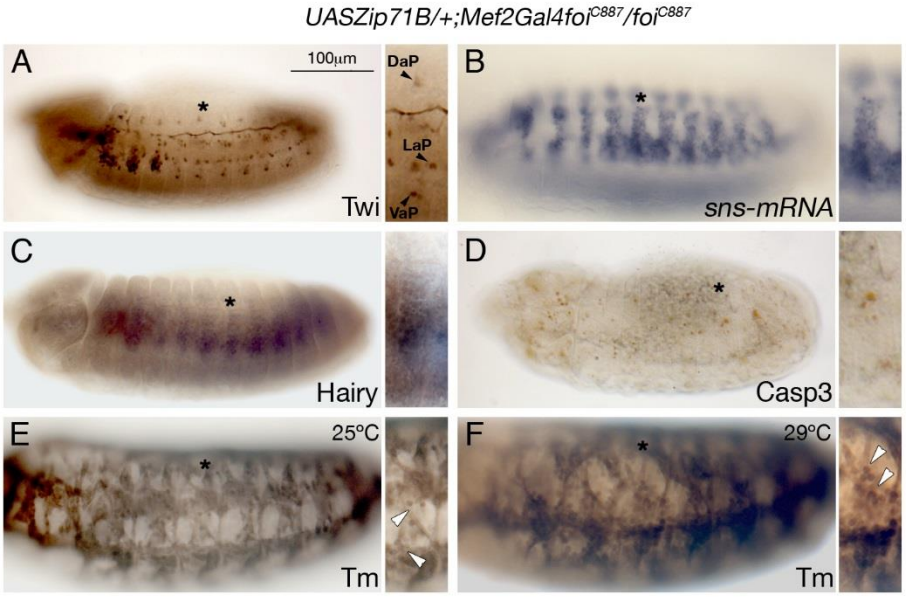

FIGURE S5, related to Figure 6. Mesodermal rescues of *foi* phenotypes with *Zip71B*

(A-F) Stages 13 (D), 14 (A-C) and 16 (E, F) *foi*^{C887} embryos with panmesodermal expression of the zinc transporter *Zip71B*. *Zip71B* causes a substantial rescue of *foi* mesodermal phenotypes as evidenced by Twi (A), *sns-mRNA* (B) and Hairy (C) patterns of expression. These conditions of *Zip71B* mesodermal expression result in a weak non fusion phenotype, as seen by the presence of unfused myoblasts at stage 16 (arrowheads in E inset), that is aggravated with the increase of temperature (arrowheads in F inset) without inducing a significant death of myoblasts (D).